Human Norovirus NS3 has RNA Helicase and Chaperoning Activities

Teng-Feng Li[1,2], Myra Hosmillo[3], Hella Schwanke[3], Ting Shu[1,2], Zhaowei Wang[1,2], Lei Yin[2], Stephen Curry[4], Ian G. Goodfellow[3], Xi Zhou[1,2,*]

[1] State Key Laboratory of Virology, Wuhan Institute of Virology, Chinese Academy of Sciences, Wuhan, Hubei, 430071, China

[2] College of Life Sciences, Wuhan University, Wuhan, Hubei, 430072, China

[3] Division of Virology, Department of Pathology, University of Cambridge, Addenbrooke's Hospital, Cambridge, CB2 0QQ, United Kingdom

[4] Department of Life Sciences, Imperial College London, London, SW7 2AZ, United Kingdom

* Address correspondence to Xi Zhou, Wuhan Institute of Virology, Chinese Academy of Sciences, 44 Xiaohongshan, Wuhan, Hubei, 430071, China. Phone: +86-27-87197727; Fax: +86-27-87197727; Email: zhouxi@wh.iov.cn

ABSTRACT

RNA remodeling proteins, including RNA helicases and chaperones, act to remodel RNA structures and/or protein-RNA interactions, and are required for all processes involving RNAs. Although many viruses encode RNA helicases and chaperones, their *in vitro* activities and their roles in infected cells largely remain elusive. Noroviruses are a diverse group of positive-stranded RNA viruses in the family *Caliciviridae*, and constitute a significant and potentially fatal threat to human health. Here we report that protein NS3 encoded by human norovirus has both ATP-dependent RNA helicase activity that unwinds RNA helices and ATP-independent RNA chaperoning activity that can remodel structured RNAs and facilitate strand-annealing. Moreover, NS3 can facilitate viral RNA synthesis *in vitro* by norovirus polymerase. NS3 may therefore play an important role in norovirus RNA replication. Lastly, we demonstrate that the RNA remodeling activity of NS3 is inhibited by guanidine hydrochloride, an FDA-approved compound and, more importantly, that it reduces the replication of norovirus replicon in cultured human cells. Altogether, these findings are the first to demonstrate the presence of RNA remodeling activities encoded by *Caliciviridae*, and highlight the functional significance of NS3 in noroviral life cycle.

41 **IMPORTANCE**

42 Noroviruses are a diverse group of positive-stranded RNA viruses, which
43 annually cause hundreds of millions of human infections and over 200,000 deaths
44 worldwide. For RNA viruses, cellular or virus-encoded RNA helicases and/or
45 chaperones have long been considered to play pivotal roles in viral life cycles.
46 However, neither RNA helicase nor chaperoning activity has been demonstrated to
47 associate with any norovirus-encoded proteins, and it is also unknown whether
48 norovirus replication requires the participation of any viral or cellular RNA
49 helicases/chaperones. We found that a norovirus protein NS3 not only has
50 ATP-dependent helicase activity, but also acts as an ATP-independent RNA chaperone.
51 And NS3 can facilitate *in vitro* viral RNA synthesis, suggesting the important role of
52 NS3 in norovirus replication. Moreover, NS3 activities can be inhibited by an
53 FDA-approved compound, which also suppresses norovirus replicon replication in
54 human cells, raising the possibility that NS3 could be a target for anti-noroviral drug
55 development.

56

57

INTRODUCTION

Noroviruses are a genetically diverse group of non-enveloped, positive-stranded RNA viruses belonging to genus *Norovirus* of the family *Caliciviridae*. They are further segregated into seven genogroups (GI-GVII), three of which cause diseases exclusively in humans (GI, GII, and GIV) (1-3). Human noroviruses (HuNoVs) are now considered the leading cause of viral gastroenteritis in humans across the globe. HuNoV infections are estimated to cause 684 million of cases of diarrheal disease, 1.1 million hospitalizations and 212 000 deaths worldwide, with an economic burden of ~60 billion dollars per year (4, 5). They are highly contagious, infecting people of all ages, with higher incidence in young children and low-income settings (4, 5). Although HuNoV infections are usually acute and self-limiting with low mortality, they often cause chronic or life-threatening infections and symptoms in immunocompromised patients and the elderly (6). As a result of their high infectivity, stability and resistance to common sanitizers, HuNoV has also been classified as Category B biodefense agents (6, 7). However, despite its substantial burden and potential threat, there is still no vaccines or antiviral drugs available to prevent or treat norovirus infection (4, 5, 8).

The noroviral genomic RNA is 7.4-7.7 kb in length and typically organized into three open reading frames (ORF1-3) (8). Exceptionally, the GV murine norovirus (MNV) has an additional ORF (ORF4) encoded within ORF2 (9, 10). The 5´ proximal ORF1 encodes a large polyprotein that is cleaved by a norovirus-encoded protease ($NS6^{Pro}$) into at least six mature nonstructural proteins, while the 3´ proximal region

of noroviral genomic RNA is transcribed into a subgenomic RNA that contains ORF2 and ORF3 that encode the major and minor structural proteins VP1 and VP2, respectively (Fig. 1A). Although these viruses have been extensively studied for decades, our understanding about the mechanisms of the nonstructural proteins involved in norovirus replication is very limited, particularly in comparison to other positive-stranded RNA viruses such as picornaviruses and flaviviruses.

For many RNA viruses, the viral RNA (vRNA) contains multiple *cis*-acting elements that play pivotal roles in vRNA replication, translation and encapsidation, during the viral life cycle (11-13). As with cellular RNA molecules, these elements are often highly structured in vRNAs and must be folded into the correct tertiary structures to be functional. However, this can be problematic because RNAs can be easily trapped in stable but misfolded intermediate states (14, 15). To avoid this, cells and viruses encode a variety of RNA remodeling proteins, such as RNA helicases and RNA chaperones, which can destabilize RNA-RNA or RNA-DNA duplexes to promote the proper folding or re-folding of RNAs (16-18). In addition, viral or cellular RNA helicases are thought to participate the unwinding of viral replicative intermediate double-stranded RNAs (vRI-dsRNAs) formed during vRNA replication, thereby allowing recycling of vRNA templates for further rounds of vRNA synthesis. RNA helicases have nucleoside triphosphatase (NTPase) activity, using the energy of NTP binding and/or hydrolysis to unwind RNA duplexes, and are believed to participate in most ATP-dependent rearrangement of structured RNAs (19). RNA chaperones are a heterogeneous group of proteins that can destabilize RNA duplexes

and promote correct RNA folding in an ATP-independent fashion (20). A wide range of RNA viruses, including flavivirus (21), picornavirus (22), alphavirus (23), coronavirus (24), reovirus (25), iflavirus (26), and alphatetravirus (27) have been found to encode their own RNA helicases and/or RNA chaperones (28).

Sequence analysis showed that the norovirus NS3 protein, also known as p41, contains signature motifs that are conserved in superfamily-3 (SF3) viral helicases such as the human enterovirus $2C^{ATPase}$ (EV71 $2C^{ATPase}$) (22), simian virus 40 (SV40) large T antigen (LTag) (29), adeno-associated virus 2 (AAV2) Rep40 (30, 31), and the human papillomavirus 18 (HPV18) E1 protein (32) (Fig. 1). Consistent with this observation, the NS3 protein encoded by Southampton virus (SHV), a GI HuNoV, has been shown to have a NTPase activity (33). In addition, norovirus NS3 has been recently reported to associate with vRI-dsRNAs in viral replication complex (vRC) and to induce vesicular structures (34-36). However, previous work has yet to demonstrate RNA helicase or chaperoning activity associated with NS3 or any other norovirus- or calicivirus-encoded proteins, or that the replication of norovirus or calicivirus requires the participation of any viral or host RNA remodeling activities. This gap hampers our understanding about the replication mechanisms of this large group of medically important human pathogens, as well as the development of anti-noroviral drugs that may specifically target viral RNA helicase/chaperoning activities.

Our previous work on enterovirus $2C^{ATPase}$ revealed that, *in vitro*, $2C^{ATPase}$ has RNA remodeling activity when expressed using a baculovirus-based expression

system (22). Here, we show that NS3 encoded by Norwalk virus (NV; genotype GI.1 HuNoV), the prototype strain of the genus *Norovirus*, also has NTP-dependent RNA helicase activity. Moreover, we demonstrate that NS3 can also act as an RNA chaperone that is able to remodel structured RNAs and facilitate strand annealing independently of NTP. We have also found that NS3 can facilitate the *in vitro* synthesis of vRNA by NV NS7/RNA-dependent RNA polymerase (RdRP) on the 3´ antigenomic template, suggesting that NS3 plays important role in norovirus RNA replication. Additionally, we have demonstrated that the guanidine hydrochloride (GuHCl), which is a U.S. FDA-approved small molecule drug and a well-known inhibitor of poliovirus $2C^{ATPase}$, is able to inhibit the RNA helicase activity of NS3 in a dose-dependent manner. More importantly, GuHCl has been further determined to inhibit the replication of NV replicon in cultured human cells, which highlights the functional significance of NS3 in noroviral life cycle.

RESULTS

NV NS3 shares similar consensus motifs and structure with other SF3 viral helicases

A comparison of the amino acid sequence of NV NS3 with members of the SF3 viral helicases, including EV71 $2C^{ATPase}$, AAV2 Rep40, SV40 LTag, and HPV18 E1, revealed that NV NS3 contains the conserved SF3 helicase A, B, and C motifs (Fig. 1B).

Since the three-dimensional (3D) structure of norovirus NS3 has not yet been reported, we modeled the NV NS3 structure using the ROBETTA server for protein structure prediction and analysis (37). The predicted model of the NV NS3 revealed that the C-terminal two thirds consisting of amino acids (a.a) at positions 122-363 (i.e. NS3ΔN) is comprised of two structurally independent domains; a helicase core (HC; a.a. 122-288) forming a central five-stranded β-sheet sandwiched by α helices on both sides, and the C-terminal domain (CTD; a.a. 289-363) comprising of several α helices. These domains are linked by flexible loops (Fig. 1C), and interestingly, demonstrates some limited similarity with the counterpart region of EV71 $2C^{ATPase}$ (22). Moreover, the predicted SF3 motifs A, B, and C of NV NS3 are nicely overlapped with the conserved SF3 motifs in these other SF3 viral helicases (Fig. 1D-F).

NV NS3 contains NTPase activity

Previous studies by Pfister and Wimmer found that bacterially expressed Southampton virus (SHV) NS3 has NTPase activity (33). To confirm whether NV

NS3 also has this activity, we expressed recombinant Maltose binding protein (MBP)-fusion NV NS3 using a baculovirus expression system , and then examined the NTPase activity by incubating MBP-NS3 with different NTPs. The hydrolysis of NTP was measured using a sensitive colorimetric assay that determines the total amount of released inorganic phosphate. As found for SHV NS3, our data showed that NV NS3 hydrolyzed all four types of NTPs (Fig. 2A). However, although SHV NS3 was reported to hydrolyze UTP less well than ATP (33), NV NS3 exhibited similar efficiency in the hydrolysis of these NTPs (Fig. 2A).

To further characterize the NTPase activity of NV NS3, we assessed the ATPase activity of MBP-NS3 under different of ATP and Mg^{2+} concentrations as well as at different pH, as ATP is the major energy source in cells. Our results showed that the amount of hydrolyzed ATP was increased with increasing amounts of ATP (Fig. 2B). In addition, our data indicates that the ATPase activity of MBP-NS3 is Mg^{2+}-dependent, since its ATP hydrolyzing activity was undetectable in absence of Mg^{2+}. Whilst the ATPase activity of MBP-NS3 was found to be optimal at 2 mM Mg^{2+} concentration, higher levels of Mg^{2+} inhibited the ATPase activity (Fig. 2C). The optimal pH for MBP-NS3 ATPase activity was found to be ~pH 7.6, but broad activity was maintained between pH 6.8 and pH 8.0 (Fig. 2D).

We also expressed MBP-fusion NV NS3 using *E. coli*, and examined its NTPase activity. We confirmed that the bacterially expressed MBP-$NS3_{NV}$ can also hydrolyze ATP and other NTPs and shows similar biochemical properties with the eukaryotically expressed MBP-$NS3_{NV}$ (data not show). Altogether, our data demonstrate that similar

183 to SHV NS3, the NV NS3 has an NTPase activity that hydrolyzes all four NTPs and is
184 Mg^{2+}-dependent.
185
186 **NV NS3 has nucleic acid helix unwinding activity**
187 To assess the potential helix unwinding activity of NV NS3, we annealed a short
188 hexachloro fluorescein (HEX)-labeled RNA and a longer unlabeled RNA to generate
189 a standard RNA helix substrate with both 5´- and 3´-single stranded protrusions (Fig.
190 3A and Table 1). The helix unwinding assay was performed by incubating the
191 standard RNA helix substrate with purified MBP-NS3 in the standard unwinding
192 reaction and then the substrate was evaluated via gel electrophoresis. As shown in Fig.
193 3A, the HEX-labeled RNA strand was released from the RNA helix substrate in the
194 presence of MBP-NS3, whereas the RNA helix substrate remained annealed when
195 MBP alone was added as a mock helicase, showing that NV NS3 can unwind the
196 RNA helix. The reactions were performed in the presence of ATP and $MgCl_2$. The
197 boiled helix substrate or the addition of MBP-fusion EV71 $2C^{ATPase}$ were used here
198 and in subsequent experiments as relevant controls for helix unwinding activity.
199 Because some viral RNA helicases have been reported to unwind DNA helices or
200 RNA-DNA hybrids (22), we sought to examine if NV NS3 can unwind nucleic acid
201 helices containing DNA. For this purpose, we constructed three helix substrates: a
202 DNA duplex (D*/D; Fig. 3B), an RNA-DNA hybrid with a longer unlabeled RNA
203 (D*/R; Fig.. 3C) or DNA strand (R*/D; Fig. 3D). Each helix substrate was reacted
204 with MBP-NS3 under the same condition as in Fig. 3A, and our results showed that

NV NS3 can efficiently unwind either of the RNA-DNA hybrids (Fig. 3C and 3D), but unwound the DNA duplexes less effectively (Fig. 3B).

We further evaluated the RNA helix unwinding activity of MBP-NS3 under different conditions. We observed that the helix unwinding activity of MBP-NS3 can be promoted by the presence of NTP, particularly ATP or GTP (Fig. 4B), indicating that NV NS3 has an RNA helicase activity. Consistent with the characterization of NS3 NTPase activity (Fig. 2C and D), the optimized helix unwinding activity of MBP-NS3 was found around 2 mM Mg^{2+} (Fig. 4C) at pH value of around 7.6 (Fig. 4D). Collectively, these findings suggest that the NV NS3 has an NTP-dependent nucleic acid helix unwinding activity.

NV NS3 directs the RNA helix unwinding from both 5′→3′ and 3′→5′ directions

The directionality of helix unwinding is a fundamental characteristic of helicases (19). Previous studies of other SF3 viral helicases have revealed that the helicase activity of EV71 $2C^{ATPase}$ has a 3′→5′ directionality, while AAV2 Rep40 and HPV18 E1 unwind helices bidirectionally (22, 31, 32). To determine the unwinding directionality of NV NS3, we generated two different RNA helix substrates: one containing a 5′ single-stranded protrusion (Fig. 5A), and the other with a 3′ single-stranded protrusion (Fig. 5B). Each substrate was subjected to helix unwinding assay in the presence of MBP-NS3. Our data showed that RNA helix substrates with either a 5′- or a 3′-protrusion could be unwound by MBP-NS3 (Fig. 5C). Moreover, the unwinding of either substrate by MBP-NS3 can be promoted by the presence of

227 ATP in a dose-dependent manner (Fig. 5D and E). Based on these observations, we
228 conclude that NV NS3 directs the unwinding of RNA helix from both 5′→3′ and
229 3′→5′ directions in an ATP-dependent manner, similar to AAV2 Rep40, another SF3
230 viral helicase (22, 31, 32).
231
232 **The conserved SF3 motif A is critical for the helicase activity of NS3**
233 The sequence analysis of NS3 indicates that NS3 contains consensus motifs that
234 are characteristic of SF3 viral helicases (Fig. 1). The motif A has been recognized as a
235 core element of the NTP binding and NTPase active site of SF3 helicases (19) and is
236 conserved in different noroviruses (Fig. 6A). Previous work by Pfister *et al.* has
237 shown that the mutation of motif A in SHV NS3 almost completely eliminated its
238 ATPase activity (33). Moreover, motif B of SF3 helicases has been reported to
239 chelates Mg^{2+} (19). We wanted to investigate if the conserved SF3 motif A or B is
240 important for the helicase activity associated with norovirus NS3. To this end, we
241 generated the GK168AA and GK168AA-DD212AA mutants of MBP-fusion NS3
242 (MBP-$NS3_{GK168AA}$ and MBP-$NS3_{GK168AA\text{-}DD212AA}$) and expressed the proteins using
243 the baculovirus expression system. In our standard helix unwinding assays we found
244 that both of the GK168AA and GK168AA-DD212AA mutations dramatically reduced
245 the helix unwinding activity of NS3 compared to wild-type (Fig. 6B). Moreover, the
246 addition of increasing concentrations of ATP had very little effect on helix unwinding
247 by MBP-$NS3_{GK168AA}$ (Fig. 6C). These findings determine that the conserved SF3
248 motifs are critical for the helicase activity of NS3.

NV NS3 also possesses an NTP-independent RNA chaperoning activity

Although we have determined that NV NS3 requires NTP to reach its optimal helix unwinding activity (Fig. 4B, 5D, and 5E) and that the conserved SF3 motif A is critical for its helicase activity (Fig. 6), we found that a portion of the helical RNA substrate could still be unwound by MBP-NS3 in the absence of ATP (Fig. 4B, 5D, and 5E). To confirm these observations and exclude the possible interference of trace amounts of NTP in the unwinding assays, we alternatively used AMP-PNP, an ATP analog that is non-hydrolysable and able to block NTPase activity. The incorporation of 5 mM AMP-PNP, instead of ATP or other NTPs, did not completely abolish the RNA helix unwinding by MBP-NS3 (Fig. 7A). Whilst both the RNA helicases and RNA chaperones possess RNA remodeling activities, and the fundamental difference between them is that the former activity requires the participation of NTP, whereas the latter is NTP-independent (20). These observations therefore suggest that NV NS3 also contains an NTP-independent RNA chaperoning activity.

RNA chaperones are generally thought to destabilize misfolded RNA secondary structures to facilitate the re-formation of more stable RNA structures (15). To further characterize the RNA chaperoning activity of NV NS3, we adapted a canonical assay, which evaluates the helix-destabilizing and annealing acceleration activities of RNA chaperones (38). In this assay, we designed and generated two 42-nt complementary RNA strands, each of which forms a defined stem-loop secondary structure; in addition, one strand is 5'-HEX labeled and the other is unlabeled, as indicated in

271 Fig. 7B. Equal amounts of the two strands were mixed and incubated in the presence
272 or absence of MBP-NS3, and the hybridization of the two strands were then
273 determined using gel shift assay. In these reactions, ATP or other NTPs were not
274 supplemented. Our data showed that the levels of the annealed hybrids were gradually
275 increased with the increasing amounts of MBP-NS3 (Fig. 7C). Moreover, although
276 minimal spontaneous hybridization could be observed in the absence of MBP-NS3
277 with prolonged incubation time (Fig. 7D, lanes 3-6), the addition of MBP-NS3 further
278 enhanced the hybridization at each time points (Fig. 7D, lanes 7-10). Altogether, our
279 results show that NV NS3 can destabilize structured RNAs and facilitate the
280 formation of a more stable RNA structure, confirming that NV NS3 is also a
281 NTP-independent RNA chaperone.
282
283 **NV NS3 promotes noroviral RNA synthesis *in vitro***
284 For positive-stranded RNA viruses, their RdRP-mediated vRNA replications
285 generate viral replicative intermediate double-stranded RNAs that could be unwound
286 by RNA helicases in order to recycle vRNA templates (39). Virus-encoded RNA
287 chaperones may help rearrange the structured RNA elements of vRNA templates,
288 thereby facilitating vRNA synthesis (25). After determining the RNA helicase and
289 chaperoning activities of NV NS3, we wanted to evaluate the potential role of NS3 in
290 norovirus RNA replication. As illustrated in Fig. 8A, we incubated a recombinantly
291 purified MBP-fusion HuNoV NS7/RdRP protein with *in vitro* transcribed RNA
292 corresponding to the 400 nts at the 3´-end of HuNoV antigenomic (-)-vRNA, which is

293 presumably the template for the initiation of (+)-vRNA synthesis, in the presence or
294 absence of WT or GK168AA mutant MBP-NS3. The reaction was not supplemented
295 with an oligonucleotide RNA primer as noroviral RNA synthesis can occur
296 primer-independently, at least *in vitro* (40). And the newly synthesized RNA was
297 detected by Northern blots using the probe specific for (+)-vRNA. Here, we observed
298 that the presence of WT MBP-NS3 promoted the NS7/RdRP-mediated production of
299 (+)-vRNA strands from the (-)-vRNA templates, and that the promoting effect of NS3
300 could be further enhanced with increasing the reaction time (Fig. 8B and 8C). On the
301 other hand, the motif A mutation mostly eliminated the promoting effect of MBP-NS3
302 on *in vitro* RNA synthesis (Fig. 8D and 8E).
303
304 **GuHCl inhibits the NTPase and RNA helix unwinding activities of NV NS3**
305 Previous studies have reported that the NTPase and RNA helicase activities of
306 enterovirus $2C^{ATPase}$ can be inhibited by GuHCl (22, 41-45), which also inhibits
307 replication of vRNA of a number of enteroviruses (46, 47). Given the similarity
308 between the consensus motifs in enterovirus $2C^{ATPase}$ and norovirus NS3, we wanted
309 to examine whether NV NS3 could also be a target for guanidine inhibition. NTPase
310 assays showed that GuHCl inhibited the ATPase activity of NV NS3 in a
311 dose-dependent manner (Fig. 9A). This result is in contrast with the previous
312 observation by Pfister and Wimmer who demonstrated that even in the presence of up
313 to 10 mM GuHCl, the ATPase activity of SHV NS3 was not inhibited (33). This
314 contrasting results might be due to the different expression strategies (eukaryotic vs.

315 prokaryotic) or the inherent biochemical properties of two NS3 proteins, which were
316 also shown to have different hydrolysis preferences for UTP (Fig. 2A) and different
317 responses to Mg^{2+} concentrations higher than 2 mM (Fig. 2C).

318 To examine if GuHCl could also inhibit the helix unwinding by NV NS3, the
319 helix unwinding reactions were performed in the presence of NS3 and increasing
320 concentrations of GuHCl. Our results showed that the presence of GuHCl inhibited
321 the helix unwinding by NS3 in a dose-dependent manner (Fig. 9B and C). Intriguingly,
322 we examined the effect of GuHCl on the RNA chaperoning activity of NV NS3 using
323 the RNA strand hybridization assay. Our data showed that the addition of GuHCl at
324 different concentrations had no obvious effect on NS3 RNA chaperoning activity (Fig.
325 9D).

326 It is important to note that the helicase activity and ATPase activity show similar
327 sensitivities to GuHCl, and the inhibitory effects due to GuHCl on helicase and
328 ATPase activities of NV NS3 are moderate, but similar to the effects observed in
329 EV71 $2C^{ATPase}$ (22). Nevertheless, these data demonstrate that GuHCl is an inhibitor
330 of the key biochemical activities of NV NS3.

331

332 **GuHCl inhibits NV replication in cultured human cells**

333 Whilst we have shown that GuHCl can inhibit the NTPase and helix unwinding
334 activities of NV NS3, we sought to determine whether GuHCl treatment can inhibit
335 HuNoV replication in cells. To this end, the effect of GuHCl on HuNoV replication
336 was evaluated by using the NV replicon system in cultured human gastric tumor

(HGT-1) cells. The levels of NV RNA in the presence of GuHCl at different concentrations were determined by real-time quantitative reverse transcription-PCR (qRT-PCR), and the expression levels of NV proteins were determined by western blotting of NV NS3. 2´-C-methylcytidine (2CMC), a nucleoside analog that has been reported to inhibit HuNoV replication (48, 49), was used as the positive control. As shown in Fig. 9E, the presence of 1.125 mM GuHCl significantly reduced the level of NV RNA to around 50% of that under mock treatment, while increasing the GuHCl concentration to 3.25 mM only moderately enhanced the inhibitory effect of GuHCl to NV RNA replication. As expected, 2CMC showed a strong inhibitory effect on NV RNA replication (Fig. 9E). We also showed that the presence of 1.125 or 3.25 mM GuHCl did not affect the viability of HGT-1 cells, as found for 2CMC treated cells, excluding the possibility that the inhibitory effect of GuHCl on NV RNA replication was due to inducing cell death (Fig. 9F). Hence, GuHCl can inhibit the replication of NV replicon at 1.125 mM in cultured human cells without apparent cytotoxicity.

352 **DISCUSSION**

353 During the life cycle of RNA viruses, cellular or virus-encoded RNA helicases or
354 chaperones are believed to facilitate correct folding or unfolding of RNA structures or
355 to separate vRI-dsRNAs for more rounds of vRNA replication (14, 15, 22). Here we
356 report for the first time that NV-encoded NS3 has both NTP-dependent RNA helicase
357 and NTP-independent RNA chaperoning activities that can unwind RNA helices, and
358 destabilize and remodel structured RNA molecules. Moreover, we have found that
359 NS3 can stimulates NS7/RdRP-mediated noroviral RNA synthesis *in vitro*, suggesting
360 that NS3 plays an important role in norovirus RNA replication. Our work has also
361 shown that GuHCl, an FDA-approved small molecule drug, can inhibit the RNA
362 helicase activity of NS3 *in vitro*, and more importantly, that this small molecule has
363 some inhibitory activity against replication of a HuNoV replicon in cultured human
364 cells.

365 The RNA remodeling activities of viral proteins are generally believed to play
366 important roles in viral life cycles (50). For instance, during vRNA replication of
367 RNA viruses, vRI-dsRNAs must be efficiently unwound, thereby releasing nascently
368 synthesized progeny vRNAs from vRNA templates. Moreover, viral genomic and
369 antigenomic RNAs contain multiple *cis*-acting elements, highly structured RNA
370 regions that usually play pivotal roles in the replication, translation, and encapsidation
371 of vRNAs (11, 51). Sometimes, a specific RNA structure required for one vRNA
372 function, like translation or encapsidation, may need disruption and refolding to
373 facilitate another vRNA function, like vRNA replication, and vice versa. For example,

374 genomic RNAs or mRNAs of some RNA viruses, including norovirus (13, 52, 53),
375 flavivirus (12), hantavirus (54), and reovirus (55), can undergo circularization,
376 resulting in the base-pairing of vRNA 5´- and 3´-ends to form panhandle-like
377 structures that may facilitate vRNA translation, encapsidation, or RdRP recruitment to
378 3´-end of vRNAs (51, 56). However, for initiation of RNA replication, these cyclized
379 vRNA structures need to be disrupted to make the 3´-end of vRNAs accessible by
380 RdRPs; an example of this type of activity is the chaperoning effect of cypovirus VP5
381 on cyclized cypoviral mRNAs (25). Viral RNA remodeling proteins may also
382 dynamically facilitate proper folding and unfolding of different vRNA structures,
383 thereby allowing vRNAs to switch among distinct functionalities.

384 For noroviruses, it has been found that their vRNAs contain multiple *cis*-acting
385 elements and RNA secondary structures, which are important for norovirus replication
386 (13, 51-53). With that in mind it is intriguing that we have observed ability of NS3 to
387 enhance NS7/RdRP-mediated noroviral RNA synthesis *in vitro*, particularly since
388 norovirus NS3 has recently been found to associate with vRI-dsRNAs in vRC on
389 intracellular membranes (34-36). These findings indicate the critical roles of NS3 in
390 norovirus RNA replication. However, owing to technical limitations, the RNA
391 remodeling activities of viral proteins have been mainly studied *in vitro*, and it is
392 difficult to imagine how the regulation of the structures and functions of vRNAs by
393 viral RNA helicases/chaperones can be investigated in detail in virus-infected cells.
394 Future advances in techniques may overcome these barriers and help understand the
395 mechanism(s) of how the RNA helicase/chaperoning activities of NS3 remodel

vRNAs at different stages of noroviral life cycle.

Interestingly, we found that the guanidine salt, GuHCl, inhibits both the ATPase and RNA helix unwinding activities of NV NS3 in a dose-dependent manner (Fig. 9), similar to the effects of the same compound on enterovirus $2C^{ATPase}$ (22, 41). Although previous work found that the ATPase activity of SHV NS3 was not inhibited by GuHCl (33), our data show that NV NS3 has some difference with SHV NS3 in terms of ATPase activity. For example, while SHV NS3 has been found to hydrolyze UTP much less well than ATP (30), NV NS3 exhibited similar hydrolysis efficiency to both ATP and UTP (Fig. 2A). Moreover, when the concentration of Mg^{2+} is higher than 2 mM, the ATPase activity of NV NS3 was inhibited in a dose-dependent manner (Fig. 2C), while that of SHV NS3 was moderately enhanced (30). It is possible that the difference between NV NS3 and SHV NS3 in ATPase activity is due to the different (eukaryotic vs. prokaryotic) expression strategies.

Virus-encoded RNA remodeling proteins, particularly helicases, have long been considered as valuable targets for antiviral compounds, because they are well conserved within or even across virus families (57). In particular, enterovirus $2C^{ATPase}$, another SF3 viral RNA helicase, has been found to be inhibited by ~1 mM GuHCl, as is enterovirus replication (22, 42-45). Using a NV replicon as model, our studies demonstrate that ~1 mM GuHCl can significantly inhibit the replication of HuNoV in cultured human cells with negligible cell toxicity (Fig. 9). Similarly, GuHCl can inhibit the replication of poliovirus at the same concentration (22). Guanidines are ubiquitously present in nature, and are categorized as organic superbases with highly

418 basic nature and notable stability, that can function as mediators of specific
419 non-covalent binding in various catalytic processes (58, 59). Due to their
420 physicochemical characteristics, guanidine molecules probably bind stably to the
421 surfaces of viral RNA remodeling proteins, such as enterovirus $2C^{ATPase}$ and HuNoV
422 NS3, and may therefore alter their conformations, electrostatic states, and/or
423 protein-protein/RNA interactions, thereby inhibiting their RNA remodeling activities.
424 In accordance with this idea, high concentrations of Mg^{2+} (> 2mM) have been found
425 to inhibit the helix unwinding by either NV NS3 (Fig. 2C) or EV71 $2C^{ATPase}$ (22).
426 GuHCl is a U.S. FDA-approved small compound drug that has been used to treat the
427 symptoms of muscle weakness and fatigability associated with Eaton-Lambert
428 syndrome
429 (http://www.accessdata.fda.gov/scripts/cder/daf/index.cfm?event=overview.process&
430 ApplNo=001546) (60, 61). Moreover, guanidine derivatives have attracted
431 widespread interest for developing drugs against various diseases, and some of them
432 have been found to be potential antivirals against hepatitis C virus (HCV), human
433 immunodeficiency virus (HIV), and flaviviruses (21, 58, 59). It is unlikely that
434 GuHCl can be directly used as an antiviral drug against HuNoV infection due to the
435 high concentration needed for inhibition of NS3 and NV replication. However, given
436 the presence of multiple derivative forms of guanidine, the syntheses and screening of
437 various guanidine derivatives and guanidine-containing compounds may help in the
438 quest for small molecules that have better inhibitory effects on HuNoV NS3 and
439 HuNoV replication.

In conclusion, this study provides the first demonstration of the RNA helicase and chaperoning activities associated with a norovirus- or calicivirus-encoded protein, and reveals that NS3 may have a direct function (in concert with the NS7/RdRP) in norovirus RNA replication. Moreover, it also provides evidence that GuHCl is an inhibitor of not only the *in vitro* RNA remodeling activities of NS3 but also the replication of HuNoV in human cells. Altogether, these findings highlight the functional significance of NS3 in noroviral life cycle, and shed new light on the understanding of norovirus replication.

MATERIALS AND METHODS

Construction of recombinant baculoviruses, and expression and purification of recombinant proteins

The generation of pFastBac HTB-MBP has been described previously (26). The cDNA of NV NS3 (GenBank Accession No. KF039736) was synthesized by Tian Yi Hui Yuan Biotech Co. (Wuhan, China), and cloned into the vector pFastBac HTB-MBP. Site-directed mutagenesis was conducted as previously described (26). The resulting plasmids were subjected to Bac-to-Bac baculovirus system to produce recombinant proteins. The primers used for NS3 plasmid construction: forward-GAATTCATGGGCCCCGAGGACCTTGCCAGGGATCTCGTG and reverse-GTCGACCTACTGGAGTTGGAACTCATCCTGTCTCTCCAT; the primers for the GK168AA and GK168AA-DD212AA of NS3 are: forward-TGTGGGCCCCC TGGTATAGCTGCTACCAAG and reverse-GTTCTGCTGCCTTGGTAGCAGCTAT ACCAG; forward-GCTGTGGGCTGCTTATGGAATGACAAAGAT and reverse-TG TATCTTTGTCATTCCATAAGCAGCCCAC.

The expression and purification of recombinant MBP alone and MBP-fusion proteins were conducted using standard procedures as previously described (25, 26). All purified proteins were quantified by BCA Protein Assay Kit (CWBIO, China) and stored at -80°C in aliquots. Proteins were separated on 10% SDS-PAGE and visualized by Coomassie blue.

Structural modeling and structural alignment analyses

The 3D structure of NV NS3 was modeled by submitting its amino acid sequence to the HMMSTR/Rosetta server [from Robetta, University of Washington (http://robetta.bakerlab.org/)]. Five models were obtained, and the best one was chosen as a template based on its score, and assessed by submitting it to the SWISS-MODEL Server [from Swiss Institute of Bioinformatics and the Biozentrum, University of Basel, Switzerland (http://siwssmodel.expasy.org)]. The Figure of the modeled NS3ΔN and the structural alignments with SV40 LTag (PDB ID code 4GDF), HPV18 E1 (PDB ID code 1TUE), and AAV2 Rep40 (PDB ID code 1U0J) were generated from coordinate files using PyMOL version 1.1 (DeLano Scientific LLC, Southern San Francisco, CA).

NTPase assay

NTPase activities were determined via measuring the released inorganic phosphate during NTP hydrolysis using a direct colorimetric assay according to our standard procedures as previously described (26). The concentrations of released inorganic phosphate were determined by matching the A620 in a known inorganic phosphate curve. All of the results given with this quantitative assay were averages of three independently repeated experiments.

Preparation of oligonucleotide helix substrates

The nucleic acid helix substrates were prepared according to our standard procedures as previous described (22). In brief, RNA, DNA or RNA-DNA hybrid

helix substrates were prepared by annealing two complementary nucleic acid strands, of which one strand was labeled at 5´-end with HEX, while the other was unlabeled. The two strands were mixed at a proper ratio in a 10 µl reaction mixture containing 25mM HEPES-KOH (pH 8.0) and 25mM NaCl. And the mixture was then heated to 95℃ for 5 min and gradually cooled to 25℃ to produce helical duplexes. All HEX-labeled DNA and RNA strands were purchased from Takara (Dalian, China), unlabeled DNA strands were synthesized by Invitrogen, and unlabeled RNA strands were *in vitro* transcribed using T7 RNA polymerase (Promega, Madison, WI). The *in vitro* transcribed RNA strands were purified by Poly-Gel RNA Extraction Kit (Omega bio-tek, Guangzhou, China) according to the manufacturer's instructions. The standard RNA helix substrate with both 5´ and 3´ protrusion was annealed using RNA1 and RNA2, the DNA helix substrate was annealed using DNA2 and DNA3, the RNA*-DNA hybrids was annealed using RNA1 and DNA1, the DNA*-RNA hybrids was annealed using DNA1 and RNA3, the 3´ protruded RNA helix was annealed using RNA1 and RNA4, and the 5´ protruded RNA helix was annealed using RNA1 and RNA5. All oligonucleotides used in this study are listed in Table 1.

Helix unwinding and RNA strand hybridization assays

Helix unwinding assay was performed according to our standard procedures as previously described (25). The reaction mixtures were electrophoresed on 15% native-PAGE gels and then scanned with a Typhoon 9500 imager (GE Healthcare, Piscataway, NJ).

528 The RNA hybridization assay was carried out according to our standard
529 procedures as previously described (25). In brief, the indicated amount of protein, 0.2
530 pmol HEX-labeled stem-loop-structured RNA strand, and 0.2 pmol unlabeled
531 stem-loop-structured RNA strand were added to reaction buffer and incubated for 1 h
532 or the indicated time. The sequences of the stem-loop-structured RNA strands are
533 given in Fig. 7B. The reaction products were resolved on 15% native-PAGE gels,
534 followed by scanning by Typhoon 9500 imager (GE Healthcare, Piscataway, NJ).
535
536 ***In vitro* RdRP assays**
537 The vRNA template was *in vitro* transcribed by T7 RNA polymerase as described
538 above. The (-)-vRNA template contains 1-400 nts of 3´-end HuNoV (-)-RNA, which
539 is complementary to 5´-end 400 nts of HuNoV (+)-RNA. The transcribed product was
540 purified by Poly-Gel RNA Extraction Kit (Omega bio-tek, Guangzhou, China)
541 according to the manufacturer's instruction. The cDNA of HuNoV NS7/RdRP
542 (GenBank Accession No. KR904238) was amplified by PCR from full-length
543 GII.4-Sydney HuNoV cDNA, which was generously provided by Dr. Linqing Zhao
544 (Capital Institute of Pediatrics, Beijing, China), and cloned into the vector the vector
545 pMAl-c2X-MBP (primers: forward-GGATCCATGGGAGGAAACACTGTCATATG
546 TGCCACCCAG and reverse-GTCGACTCACTCGACGCCATCTTCATTCACAAA
547 ACTGGG). The recombinant MBP-fusion NS7/RdRP was purified as described
548 above. The RdRP assay was performed as previously described with minor
549 modification. In brief, indicated amounts of MBP-NS3 were included in 10 µl

reactions containing 50mM HEPES-KOH (pH7.5), 12.5mM KCl, 5mM $MgCl_2$, 5mM DTT, 20U RNasin (Promega), and 5mM NTPs. MBP-NS3 was included in the reaction mix with or without 10 pmol NS7/RdRP at 30℃ for the indicated time. After that, the reaction was terminated by 2×loading buffer (20% 10×MOPS running buffer, 10% glycerol, 50% formamide, 20% formaldehyde and 0.05% bromophenol blue), and then denatured at 65℃ for 10min. The samples were electrophoresed on 1.5% agarose-formaldehyde denaturing gels, and transferred onto N+ nylon membranes (Roche). The RdRP products were detected via Northern blots that were performed according to our standard procedures (62). The probe for Northern blots was listed in Table 1.

Assessment of GuHCl treatment in HuNoV-replicon harboring cells

A baby hamster kidney cell line harbouring the NV replicon, provided by Dr. Kim Green (National Institutes of Health, Bethesda, MD), was used as a source of viral VPg-linked RNA (63). Total RNA was isolated from the BHK-NV replicon containing cell line and transfected into HGT-1 (64). The transfected cells were placed under selection using 1mg/ml of G418 and clonal populations were generated by limiting dilution. The levels of viral RNA determined by qRT-PCR as described and a single clone selected for future use, referred to as HGT-NV.

To examine the effect of GuHCl on NV replication, HGT-NV cells were seeded in 96-well plate at 1,000 cells per well without G418. HGT-NV cells were immediately incubated with media containing various levels of GuHCl or 2CMC as a control. Cells were incubated at 37°C in 5% CO_2 for 3 days. The effect of GuHCl treatment on

573 HuNoV replicon RNA was then evaluated by qRT-PCR as described (65) and western
574 blot using rabbit polyclonal antisera to norovirus NS3. In addition, the effect of
575 GuHCl on cell viability was determined using CellTiter-Blue (Promega) according to
576 the manufacturer's instructions.
577
578
579
580

ACKNOWLEDGMENTS

We thank Dr. Linqing Zhao (Beijing, China) for generously providing reagents, and Drs. Linqing Zhao and Huimin Yan (Wuhan, China) for helpful discussions.

This work was supported by the National Natural Science Foundation of China (NSFC) - Excellent Young Scientists Fund (grant No. 31522004 to X.Z.), the Newton Advanced Fellowship from the UK Academy of Medical Sciences and NSFC (No. 3161101464 to X.Z. and S.C.), the NSFC grant No. 31670161 (to X.Z.), the Strategic Priority Research Program of Chinese Academy of Sciences (No. XDPB0301 to X.Z.), the National High-Tech R&D Program of China (863 Program; grant No. 2015AA020939 to X.Z.), the National Basic Research Program of China (973 Program; grant No. 2014CB542603 to X.Z.), and the Distinguished Young Scientists Fund of Hubei Province (grant No. 2016CFA045 to X.Z.). The funders had no role in study design, data collection and analysis, decision to publish, or preparation of the manuscript.

603 **REFERENCES**

604 1. **Zheng, D. P., T. Ando, R. L. Fankhauser, R. S. Beard, R. I. Glass, and S. S. Monroe.** 2006.
605 Norovirus classification and proposed strain nomenclature. Virology **346:**312-323.
606 2. **Fankhauser, R. L., J. S. Noel, S. S. Monroe, T. Ando, and R. I. Glass.** 1998. Molecular
607 epidemiology of "Norwalk-like viruses" in outbreaks of gastroenteritis in the United States. J
608 Infect Dis **178:**1571-1578.
609 3. **Vinje, J.** 2015. Advances in laboratory methods for detection and typing of norovirus. J Clin
610 Microbiol **53:**373-381.
611 4. **Kaufman, S. S., K. Y. Green, and B. E. Korba.** 2014. Treatment of norovirus infections:
612 moving antivirals from the bench to the bedside. Antiviral Res **105:**80-91.
613 5. **Arias, A., E. Emmott, S. Vashist, and I. Goodfellow.** 2013. Progress towards the prevention
614 and treatment of norovirus infections. Future Microbiol **8:**1475-1487.
615 6. **Karst, S. M.** 2010. Pathogenesis of noroviruses, emerging RNA viruses. Viruses **2:**748-781.
616 7. **Leen, E. N., F. Sorgeloos, S. Correia, Y. Chaudhry, F. Cannac, C. Pastore, Y. Xu, S. C.**
617 **Graham, S. J. Matthews, I. G. Goodfellow, and S. Curry.** 2016. A Conserved Interaction
618 between a C-Terminal Motif in Norovirus VPg and the HEAT-1 Domain of eIF4G Is Essential
619 for Translation Initiation. PLoS Pathog **12:**e1005379.
620 8. **Karst, S. M., C. E. Wobus, I. G. Goodfellow, K. Y. Green, and H. W. Virgin.** 2014.
621 Advances in norovirus biology. Cell Host Microbe **15:**668-680.
622 9. **McFadden, N., D. Bailey, G. Carrara, A. Benson, Y. Chaudhry, A. Shortland, J. Heeney,**
623 **F. Yarovinsky, P. Simmonds, A. Macdonald, and I. Goodfellow.** 2011. Norovirus regulation
624 of the innate immune response and apoptosis occurs via the product of the alternative open
625 reading frame 4. PLoS Pathog **7:**e1002413.
626 10. **Thorne, L., D. Bailey, and I. Goodfellow.** 2012. High-resolution functional profiling of the
627 norovirus genome. J Virol **86:**11441-11456.
628 11. **Alhatlani, B., S. Vashist, and I. Goodfellow.** 2015. Functions of the 5' and 3' ends of
629 calicivirus genomes. Virus Res **206:**134-143.
630 12. **Hahn, C. S., Y. S. Hahn, C. M. Rice, E. Lee, L. Dalgarno, E. G. Strauss, and J. H. Strauss.**
631 1987. Conserved elements in the 3' untranslated region of flavivirus RNAs and potential
632 cyclization sequences. J Mol Biol **198:**33-41.
633 13. **McFadden, N., A. Arias, I. Dry, D. Bailey, J. Witteveldt, D. J. Evans, I. Goodfellow, and P.**
634 **Simmonds.** 2013. Influence of genome-scale RNA structure disruption on the replication of
635 murine norovirus--similar replication kinetics in cell culture but attenuation of viral fitness in
636 vivo. Nucleic Acids Res **41:**6316-6331.
637 14. **Bleichert, F., and S. J. Baserga.** 2007. The long unwinding road of RNA helicases.
638 Molecular cell **27:**339-352.
639 15. **Jarmoskaite, I., and R. Russell.** 2014. RNA helicase proteins as chaperones and remodelers.
640 Annual review of biochemistry **83:**697-725.
641 16. **Grohman, J. K., R. J. Gorelick, C. R. Lickwar, J. D. Lieb, B. D. Bower, B. M. Znosko,**
642 **and K. M. Weeks.** 2013. A guanosine-centric mechanism for RNA chaperone function.
643 Science **340:**190-195.
644 17. **Rajkowitsch, L., D. Chen, S. Stampfl, K. Semrad, C. Waldsich, O. Mayer, M. F. Jantsch,**
645 **R. Konrat, U. Blasi, and R. Schroeder.** 2007. RNA chaperones, RNA annealers and RNA

helicases. RNA Biol **4:**118-130.

18. **Lorsch, J. R.** 2002. RNA chaperones exist and DEAD box proteins get a life. Cell **109:**797-800.
19. **Kadare, G., and A. L. Haenni.** 1997. Virus-encoded RNA helicases. J Virol **71:**2583-2590.
20. **Musier-Forsyth, K.** 2010. RNA remodeling by chaperones and helicases. RNA Biol **7:**632-633.
21. **Frick, D. N.** 2007. The hepatitis C virus NS3 protein: a model RNA helicase and potential drug target. Curr Issues Mol Biol **9:**1-20.
22. **Xia, H., P. Wang, G. C. Wang, J. Yang, X. Sun, W. Wu, Y. Qiu, T. Shu, X. Zhao, L. Yin, C. F. Qin, Y. Hu, and X. Zhou.** 2015. Human Enterovirus Nonstructural Protein 2CATPase Functions as Both an RNA Helicase and ATP-Independent RNA Chaperone. PLoS Pathog **11:**e1005067.
23. **Karpe, Y. A., P. P. Aher, and K. S. Lole.** 2011. NTPase and 5'-RNA triphosphatase activities of Chikungunya virus nsP2 protein. PLoS One **6:**e22336.
24. **Lee, N. R., H. M. Kwon, K. Park, S. Oh, Y. J. Jeong, and D. E. Kim.** 2010. Cooperative translocation enhances the unwinding of duplex DNA by SARS coronavirus helicase nsP13. Nucleic Acids Res **38:**7626-7636.
25. **Yang, J., Z. Cheng, S. Zhang, W. Xiong, H. Xia, Y. Qiu, Z. Wang, F. Wu, C. F. Qin, L. Yin, Y. Hu, and X. Zhou.** 2014. A cypovirus VP5 displays the RNA chaperone-like activity that destabilizes RNA helices and accelerates strand annealing. Nucleic Acids Res **42:**2538-2554.
26. **Cheng, Z., J. Yang, H. Xia, Y. Qiu, Z. Wang, Y. Han, X. Xia, C. F. Qin, Y. Hu, and X. Zhou.** 2013. The nonstructural protein 2C of a Picorna-like virus displays nucleic acid helix destabilizing activity that can be functionally separated from its ATPase activity. J Virol **87:**5205-5218.
27. **Wang, Q., Y. Han, Y. Qiu, S. Zhang, F. Tang, Y. Wang, J. Zhang, Y. Hu, and X. Zhou.** 2012. Identification and characterization of RNA duplex unwinding and ATPase activities of an alphatetravirus superfamily 1 helicase. Virology **433:**440-448.
28. **Yang, J., H. Xia, Q. Qian, and X. Zhou.** 2015. RNA chaperones encoded by RNA viruses. Virologica Sinica **30:**401-409.
29. **Li, D., R. Zhao, W. Lilyestrom, D. Gai, R. Zhang, J. A. DeCaprio, E. Fanning, A. Jochimiak, G. Szakonyi, and X. S. Chen.** 2003. Structure of the replicative helicase of the oncoprotein SV40 large tumour antigen. Nature **423:**512-518.
30. **Zarate-Perez, F., M. Bardelli, J. W. Burgner, 2nd, M. Villamil-Jarauta, K. Das, D. Kekilli, J. Mansilla-Soto, R. M. Linden, and C. R. Escalante.** 2012. The interdomain linker of AAV-2 Rep68 is an integral part of its oligomerization domain: role of a conserved SF3 helicase residue in oligomerization. PLoS Pathog **8:**e1002764.
31. **Collaco, R. F., V. Kalman-Maltese, A. D. Smith, J. D. Dignam, and J. P. Trempe.** 2003. A biochemical characterization of the adeno-associated virus Rep40 helicase. The Journal of biological chemistry **278:**34011-34017.
32. **Lin, B. Y., A. M. Makhov, J. D. Griffith, T. R. Broker, and L. T. Chow.** 2002. Chaperone Proteins Abrogate Inhibition of the Human Papillomavirus (HPV) E1 Replicative Helicase by the HPV E2 Protein. Molecular and Cellular Biology **22:**6592-6604.
33. **Pfister, T., and E. Wimmer.** 2001. Polypeptide p41 of a Norwalk-like virus is a nucleic acid-independent nucleoside triphosphatase. J Virol **75:**1611-1619.

34. **Eden, J. S., M. M. Tanaka, M. F. Boni, W. D. Rawlinson, and P. A. White.** 2013. Recombination within the pandemic norovirus GII.4 lineage. J Virol **87:**6270-6282.

35. **Bull, R. A., M. M. Tanaka, and P. A. White.** 2007. Norovirus recombination. J Gen Virol **88:**3347-3359.

36. **Cotton, B. T., J. L. Hyde, S. T. Sarvestani, S. V. Sosnovtsev, K. Y. Green, P. A. White, and J. M. Mackenzie.** 2017. The Norovirus NS3 Protein Is a Dynamic Lipid- and Microtubule-Associated Protein Involved in Viral RNA Replication. J Virol **91**.

37. **Bystroff, C., and Y. Shao.** 2002. Fully automated ab initio protein structure prediction using I-SITES, HMMSTR and ROSETTA. Bioinformatics **18 Suppl 1:**S54-61.

38. **DeStefano, J. J., and O. Titilope.** 2006. Poliovirus protein 3AB displays nucleic acid chaperone and helix-destabilizing activities. J Virol **80:**1662-1671.

39. **Lam, A. M., and D. N. Frick.** 2006. Hepatitis C virus subgenomic replicon requires an active NS3 RNA helicase. J Virol **80:**404-411.

40. **Fukushi, S., S. Kojima, R. Takai, F. B. Hoshino, T. Oka, N. Takeda, K. Katayama, and T. Kageyama.** 2004. Poly(A)- and Primer-Independent RNA Polymerase of Norovirus. Journal of Virology **78:**3889-3896.

41. **Pfister, T., and E. Wimmer.** 1999. Characterization of the nucleoside triphosphatase activity of poliovirus protein 2C reveals a mechanism by which guanidine inhibits poliovirus replication. The Journal of biological chemistry **274:**6992-7001.

42. **Pincus, S. E., D. C. Diamond, E. A. Emini, and E. Wimmer.** 1986. Guanidine-selected mutants of poliovirus: mapping of point mutations to polypeptide 2C. J Virol **57:**638-646.

43. **Loddo, B., W. Ferrari, G. Brotzu, and A. Spanedda.** 1962. In vitro inhibition of infectivity of polio viruses by guanidine. Nature **193:**97-98.

44. **Caliguiri, L. A., and I. Tamm.** 1968. Action of guanidine on the replication of poliovirus RNA. Virology **35:**408-417.

45. **Loddo, B., S. Muntoni, A. Spanedda, G. Brotzu, and W. Ferrari.** 1963. Guanidine conditioned infectivity of ribonucleic acid extracted from a strain of guanidine-dependent polio-1-virus. Nature **197:**315.

46. **Lyons, T., K. E. Murray, A. W. Roberts, and D. J. Barton.** 2001. Poliovirus 5'-terminal cloverleaf RNA is required in cis for VPg uridylylation and the initiation of negative-strand RNA synthesis. J Virol **75:**10696-10708.

47. **Steil, B. P., and D. J. Barton.** 2009. Conversion of VPg into VPgpUpUOH before and during poliovirus negative-strand RNA synthesis. J Virol **83:**12660-12670.

48. **Rocha-Pereira, J., D. Jochmans, Y. Debing, E. Verbeken, M. S. Nascimento, and J. Neyts.** 2013. The viral polymerase inhibitor 2'-C-methylcytidine inhibits Norwalk virus replication and protects against norovirus-induced diarrhea and mortality in a mouse model. J Virol **87:**11798-11805.

49. **Rocha-Pereira, J., D. Jochmans, K. Dallmeier, P. Leyssen, R. Cunha, I. Costa, M. S. Nascimento, and J. Neyts.** 2012. Inhibition of norovirus replication by the nucleoside analogue 2'-C-methylcytidine. Biochemical and biophysical research communications **427:**796-800.

50. **Zuniga, S., I. Sola, J. L. Cruz, and L. Enjuanes.** 2009. Role of RNA chaperones in virus replication. Virus Res **139:**253-266.

51. **Lopez-Manriquez, E., S. Vashist, L. Urena, I. Goodfellow, P. Chavez, J. E. Mora-Heredia,**

C. Cancio-Lonches, E. Garrido, and A. L. Gutierrez-Escolano. 2013. Norovirus genome circularization and efficient replication are facilitated by binding of PCBP2 and hnRNP A1. J Virol **87:**11371-11387.

52. **Yunus, M. A., X. Lin, D. Bailey, I. Karakasiliotis, Y. Chaudhry, S. Vashist, G. Zhang, L. Thorne, C. C. Kao, and I. Goodfellow.** 2015. The murine norovirus core subgenomic RNA promoter consists of a stable stem-loop that can direct accurate initiation of RNA synthesis. J Virol **89:**1218-1229.

53. **Lin, X., L. Thorne, Z. Jin, L. A. Hammad, S. Li, J. Deval, I. G. Goodfellow, and C. C. Kao.** 2015. Subgenomic promoter recognition by the norovirus RNA-dependent RNA polymerases. Nucleic Acids Res **43:**446-460.

54. **Raju, R., and D. Kolakofsky.** 1989. The ends of La Crosse virus genome and antigenome RNAs within nucleocapsids are base paired. J Virol **63:**122-128.

55. **Tortorici, M. A., B. A. Shapiro, and J. T. Patton.** 2006. A base-specific recognition signal in the 5' consensus sequence of rotavirus plus-strand RNAs promotes replication of the double-stranded RNA genome segments. RNA **12:**133-146.

56. **Chen, D., and J. T. Patton.** 1998. Rotavirus RNA replication requires a single-stranded 3' end for efficient minus-strand synthesis. J Virol **72:**7387-7396.

57. **Kwong, A. D., B. G. Rao, and K. T. Jeang.** 2005. Viral and cellular RNA helicases as antiviral targets. Nature reviews. Drug discovery **4:**845-853.

58. **Saczewski, F., and L. Balewski.** 2009. Biological activities of guanidine compounds. Expert Opin Ther Pat **19:**1417-1448.

59. **Saczewski, F., and L. Balewski.** 2013. Biological activities of guanidine compounds, 2008 - 2012 update. Expert Opin Ther Pat **23:**965-995.

60. **Oh, S. J., Y. W. Lee, and E. Rutsky.** 1977. Eaton-Lambert syndrome: reflex improvement with guanidine. Arch Phys Med Rehabil **58:**457-459.

61. **O, S. J., and K. W. Kim.** 1973. Guanidine hydrochloride in the Eaton-Lambert syndrome. Electrophysiologic improvement. Neurology **23:**1084-1090.

62. **Wang, Z., D. Wu, Y. Liu, X. Xia, W. Gong, Y. Qiu, J. Yang, Y. Zheng, J. Li, Y. F. Wang, Y. Xiang, Y. Hu, and X. Zhou.** 2015. Drosophila Dicer-2 has an RNA interference-independent function that modulates Toll immune signaling. Sci Adv **1:**e1500228.

63. **Chang, K. O., S. V. Sosnovtsev, G. Belliot, A. D. King, and K. Y. Green.** 2006. Stable expression of a Norwalk virus RNA replicon in a human hepatoma cell line. Virology **353:**463-473.

64. **Laboisse, C. L., C. Augeron, M. H. Couturier-Turpin, C. Gespach, A. M. Cheret, and F. Potet.** 1982. Characterization of a newly established human gastric cancer cell line HGT-1 bearing histamine H2-receptors. Cancer Res **42:**1541-1548.

65. **Kageyama, T., S. Kojima, M. Shinohara, K. Uchida, S. Fukushi, F. B. Hoshino, N. Takeda, and K. Katayama.** 2003. Broadly reactive and highly sensitive assay for Norwalk-like viruses based on real-time quantitative reverse transcription-PCR. J Clin Microbiol **41:**1548-1557.

777 **FIGURE LEGENDS**

778 **Fig. 1. Norovirus NS3 is similar with other virus-encoded SF3 helicases in**
779 **consensus motifs and protein structures.** (A) The genomic RNA of norovirus is
780 depicted, which contains three ORFs (1, 2, and 3). The 5' proximal ORF1 encodes a
781 polyprotein that is subsequently self-cleaved into six nonstructural proteins (NS1/2,
782 NS3, NS4, NS5/VPg, NS6^{Pro}, and NS7/RdRP) by viral protease NS6^{Pro}. The ORF2
783 and ORF3 encode structural proteins VP1 and VP2, respectively. (B) Sequence
784 alignments of the helicase core domains of NV NS3 and other SF3 viral helicases,
785 including EV71 2C^{ATPase}, SV40 LTag, HPV18 E1, and AAV2 Rep40. The SF3
786 consensus motifs A, B, and C were indicated. (C) The structure of NV NS3 without its
787 N-terminal domain (NS3ΔN) was predicted by the HMMSTR/Rosetta server. NS3ΔN
788 containing the middle helicase core (HC) domain and the C-terminal domain (CTD) is
789 shown in green. The SF3 motifs A, B, and C are indicated and highlighted in red.
790 (D-F) Structural alignments of NV NS3ΔN (green) and SV40 LTag, HPV18E1, or
791 AAV2 Rep40 (cyan). The N-terminal domain of E2 binding to HPV18 E1 is shown in
792 brown. The SF3 motifs A, B, and C of these viral helicases are highlighted in blue.

793

794 **Fig. 2. NV NS3 has NTPase activity.** (A) MBP-NS3 was reacted with the indicated
795 NTP. The NTPase activity was measured as nanomoles of released inorganic
796 phosphate. (B-D) The NTPase activity of MBP-NS3 was determined at the indicated
797 concentrations of ATP (B), at the indicated concentrations of Mg^{2+} (C), or at the
798 indicated pH (D). For (B and C), the MBP alone was used as the negative control. For

(A-D), error bars represent standard deviation (SD) values from three separate experiments.

Fig. 3. NV NS3 has nucleic acid helix unwinding activity. (A) The standard RNA/RNA helix (R*/R substrate) is illustrated in the upper panel. 0.1 pmol R*/R substrate was reacted with 20 pmol each indicated protein. Non-boiled reaction mixture (lane 1) and the reaction mixture with MBP alone (lane 3) were used as negative controls, boiled reaction mixture (lane 2) and the reaction mixture with purified MBP-fusion EV71 $2C^{ATPase}$ (lane 5) were used as positive controls. (B-D) DNA/DNA helix (D*/D substrate), DNA/RNA hybrid helix (D*/R), and RNA/DNA hybrid helix (R*/D) are illustrated in each upper panel. 0.1 pmol of each indicated substrate was reacted with 20 pmol each indicted protein. For (B-D), lane 1, non-boiled reaction mixture; lane 2, boiled reaction mixture; lane 3, reaction mixture with purified MBP-fusion NS3; lane 4, reaction mixture with purified MBP-fusion EV71 $2C^{ATPase}$. The helix unwinding was detected via gel electrophoresis and scanning on a Typhoon 9500 imager. Asterisks indicate the HEX-labeled strands.

Fig. 4. Biochemical characterization of RNA helix unwinding activity of NV NS3. (A) Illustration of the standard RNA helix (R*/R) substrate. (B-D) 0.1 pmol R*/R substrate was reacted with 20 pmol MBP-NS3 in the absence or presence of individual NTP (B), increasing concentrations of Mg^{2+} (C), or different pH values (D) as indicated. Non-boiled (lane 1) or boiled (lane 2) reaction mixture was used as

821 negative or positive control. Asterisks indicate the HEX-labeled strands. The helix
822 unwinding activity was detected via gel electrophoresis and scanning on a Typhoon
823 9500 imager.
824
825 **Fig. 5. NV NS3 unwinds RNA helix in a bidirectional manner.** (A and B)
826 Schematic illustration of the RNA helix substrate with the 5' single-stranded
827 protrusion (A) or 3' single-stranded protrusion (B). Asterisks indicate the
828 HEX-labeled strands. (C) MBP-NS3 (20 pmol) was incubated with 5' single-stranded
829 protruded (lane 3) or 3' single-stranded protruded (lane 6) RNA helix substrate (0.1
830 pmol). Non-boiled (lanes 1 and 4) or boiled reaction mixtures (lanes 2 and 5) were
831 used as negative or positive controls. (D and E) MBP-NS3 (20 pmol) was reacted
832 with 5'-protruded (D) or 3'-protruded RNA helix substrate (E) in the presence of
833 indicated concentrations of ATP. The helix unwinding was detected as described in
834 Fig. 3.
835
836 **Fig. 6. The SF3 motif A is critical for the helicase activity of NV NS3.** (A) Amino
837 acids sequence alignment of NV NS3, SHV NS3, and MNV NS3. The SF3 consensus
838 motifs A, B, and C were indicated. (B) The standard RNA helix (R*/R) substrate (0.1
839 pmol) was reacted with 20 pmol wild-type (WT) (lane 4), GK168AA (lane 5), or
840 GK168AA-DD212AA (lane 6) MBP-NS3. Non-boiled reaction mixture (lane 1) and
841 the reaction mixture with MBP alone addition (lane 3) were used as negative controls;
842 the boiled reaction mixture (lane 2) was used as positive control. (C) The standard

843 RNA helix (R*/R) substrate (0.1 pmol) was reacted with 20 pmol GK168AA mutant
844 MBP-NS3 in the presence of indicated concentrations of ATP. For (B and C), asterisks
845 indicate the HEX-labeled strands.
846
847 **Fig. 7. NV NS3 has RNA chaperoning activity to destabilize structured RNA**
848 **strands and promote annealing.** (A) The standard RNA helix (R*/R) substrate (0.1
849 pmol) was reacted with 20 pmol MBP-NS3 in the absence or presence of 5 mM ATP
850 or ATP analog (AMP-PNP) as indicated. Lane 1, non-boiled reaction mixture; lane 2,
851 boiled reaction mixture; lane 3, the reaction mixture with MBP-NS3 in the absence of
852 ATP; lanes 4-5, the reaction mixture with MBP-NS3 in the presence of AMP-PNP or
853 ATP. (B) Schematic illustrations of the stem-loop structures of the two complementary
854 42-nt RNA strands. Asterisk indicates the HEX-labeled strand. (C) The two strands
855 were 1:1 mixed (0.1 pmol each) and reacted with indicated amount of MBP-NS3. (D)
856 The hybridization assay as in (C) was conducted in the absence (lanes 3-6) or
857 presence (lanes 7-10) of 20 pmol MBP-NS3 for indicated reaction times. For (C and
858 D), the pre-annealed (lane 1) or boiled (lane 2) strands were used as positive or
859 negative control, respectively. The hybridized and free strands are indicated.
860
861 **Fig. 8. NV NS3 facilitates noroviral RNA synthesis *in vitro*.** (A) Schematic
862 illustration of the experimental procedures. (B and D) The *in vitro* transcribed NV
863 3'-end 1-400 nts of (-)-vRNA template was incubated with 10 pmol recombinant
864 NS7/RdRP and NTP mix in the absence or presence of 10 pmol MBP-NS3 (B) or

865 MBP-NS3$_{GK168AA}$ (D) at 30 °C for 30, 60 or 90 min as indicated. The reaction
866 products were detected by Northern blots. (C and E) The synthesized (+)-RNA
867 products in (B and D) were quantified via Bio-Rad Quantity One software. The
868 relative RNA production was determined by comparing the level of RNA products in
869 presence of MBP-NS3 at each indicated time point with that in the absence of NS3 at
870 30 min (lane 2). The error bars represent SD values from three separate experiments.
871
872 **Fig. 9. GuHCl inhibits the biochemical activities of NV NS3.** (A) The NTPase
873 activity of MBP-NS3 was measured as nanomoles of released inorganic phosphate in
874 the presence of indicated concentrations (0-10 mM) of GuHCl. MBP alone was used
875 as the negative control. (B) The standard RNA helix (R*/R) substrate is illustrated in
876 the upper panel. 0.1 pmol R*/R substrate was reacted with 20 pmol MBP-NS3 in the
877 presence of indicated concentrations (0-10 mM) of GuHCl. Native (lane 1) or boiled
878 (lane 2) reaction mixture was used as negative or positive control, respectively. The
879 helix unwinding was detected via gel electrophoresis and scanning on a Typhoon
880 9500 imager. Asterisk indicates the HEX-labeled strand. (C) The unwinding activities
881 under different GuHCl concentrations were plotted as a percentage of the released
882 RNA from the total RNA helix substrate (Y-axis) at each indicated GuHCl
883 concentration (X-axis) via Bio-Rad Quantity One software. The error bars represent
884 standard deviation values from three separate experiments. (D) The two strands in Fig.
885 7B were 1:1 mixed (0.1 pmol each) and reacted with 10 pmol MBP-NS3 for 30 min in
886 presence of different concentrations of GuHCl in the absence of NTP. The

hybridization of the two strand was detected via gel electrophoresis and scanning on a Typhoon 9500 imager. The pre-annealed (lane 1) or boiled (lane 2) reaction mixture was used as positive or negative control, respectively. The hybridized and free strands are indicated. (E) The effect of GuHCl or 2-CMC on Norwalk virus RNA levels was determined by examining the impact on NV replicon RNA levels in HGT-NV cells following 3 days of treatment. HGT-NV cells were treated with the indicated levels of either GuHCl or 2-CMC and the levels of viral RNA calculated as a percentage of mock-treated control. (F) HGT-NV cells were treated as in (D) and the number of viable cells were determined. The cell viability was calculated as a percentage of mock-treated control. The error bars represent SD (*n*=3). Statistical significance was determined using an unpaired t-test. The experiment was repeated at least two independent times, with one representative data set presented.

909 **TABLE**

910 **Table 1** List of oligonucleotides.

Oligonuleotide	Sequence(5'-3')
RNA1	***CAUUAUCGGAUAGUGGAACCUAGCUUCGACUAUCGGAUAAUC**
RNA2	AAUAAAGAUUAUCCGAUAGUCGAAGCUAGGUUCCACUAUCCGAUAAUGAAAUAA
RNA3	UGUAGUGCUGCCAUGGUGUGGUGGUGGUGGUUGUGGUGGAGCUACGAAC
RNA4	GAUUAUCCGAUAGUCGAAGCUAGGUUCCACUAUCCGAUAAUGAAAUAA
RNA5	AAUAAAGAUUAUCCGAUAGUCGAAGCUAGGUUCCACUAUCCGAUAAUG
DNA1	AATAAAGATTATCCGATAGTCGAAGCTAGGTTCCACTATCCGATAATGAAATAA
DNA2	***CACCACAACCACCACCACCACACCATGG**
DNA3	TGTAGTGCTGCCATGGTGTGGTGGTGGTGGTTGTGGTGGAGCTACGAAC
Probe	GUGAAUGAAGAUGGCGUCUAACGGCGCUUCCGCUGCCGCUGUUGCCAACAGCAACAACGACAUCGCAAAAUCUUCAAGUGACGGUGUGUUUUCUAACAUGGCUGUCACUUUUAAGCGGGCCCUCGGGGCGCGGCCUAAAC

911 *indicate HEX labeled strand.

A

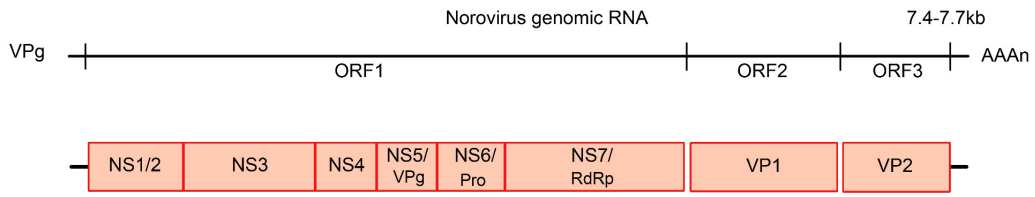

B

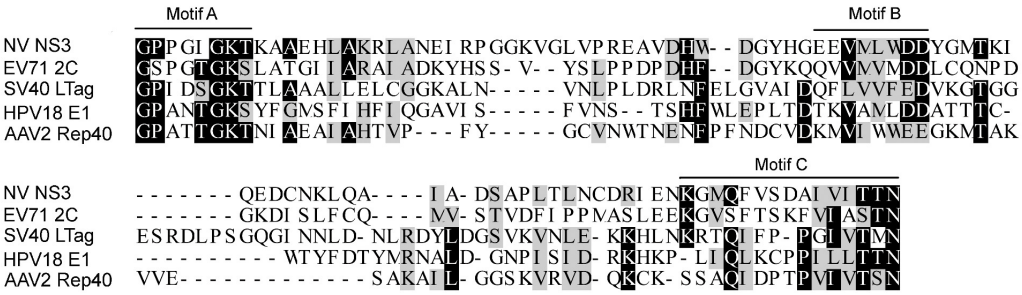

C

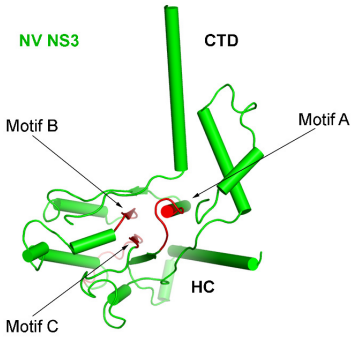

D

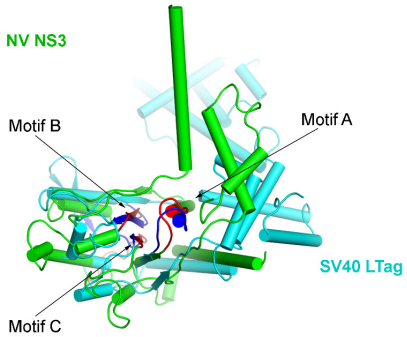

E

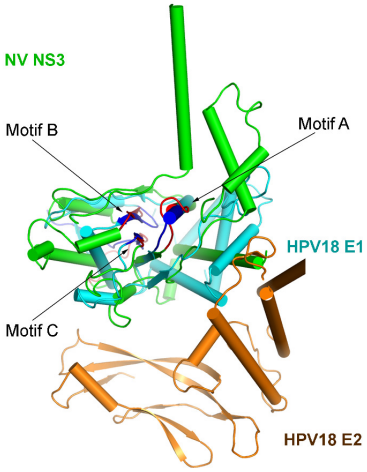

F

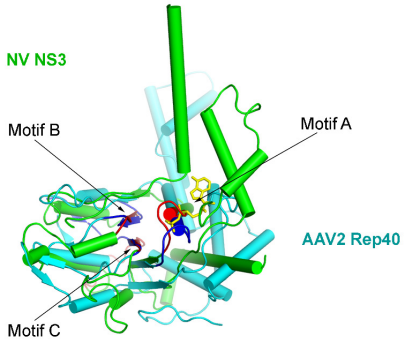

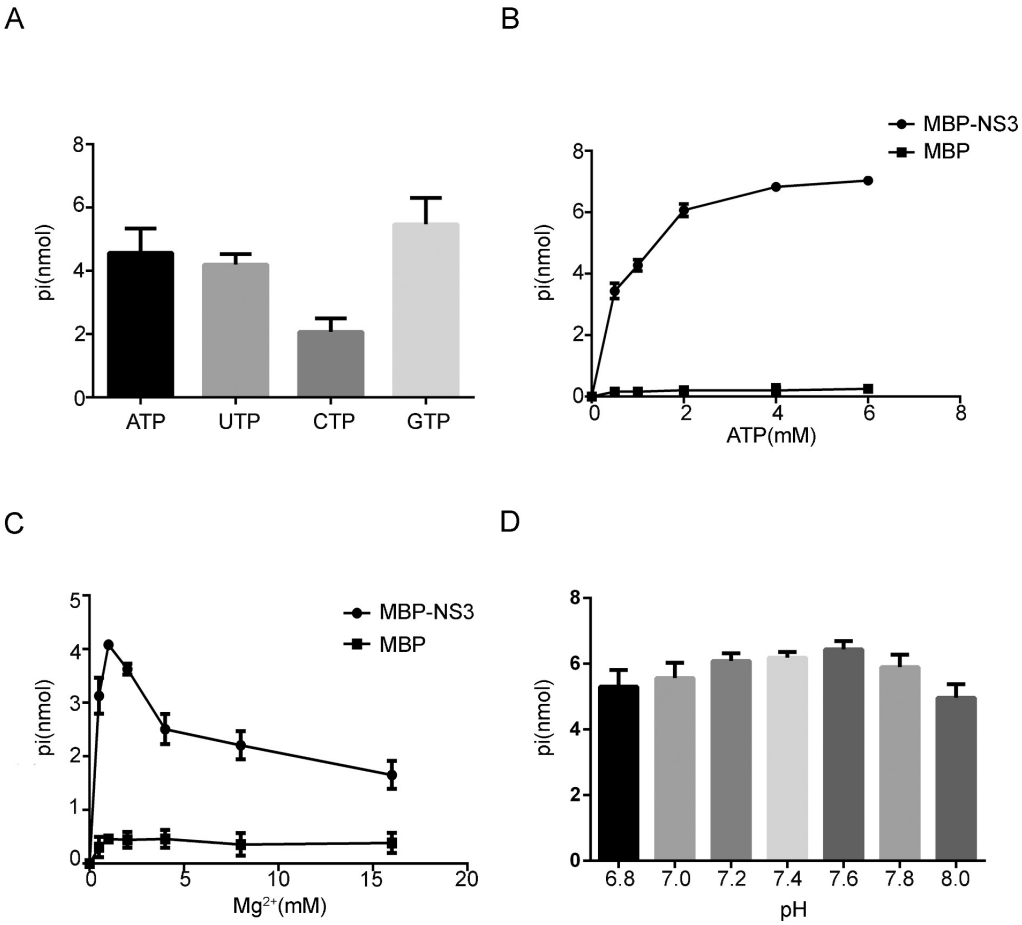

Journal of Virology
JVI
Journal of Virology

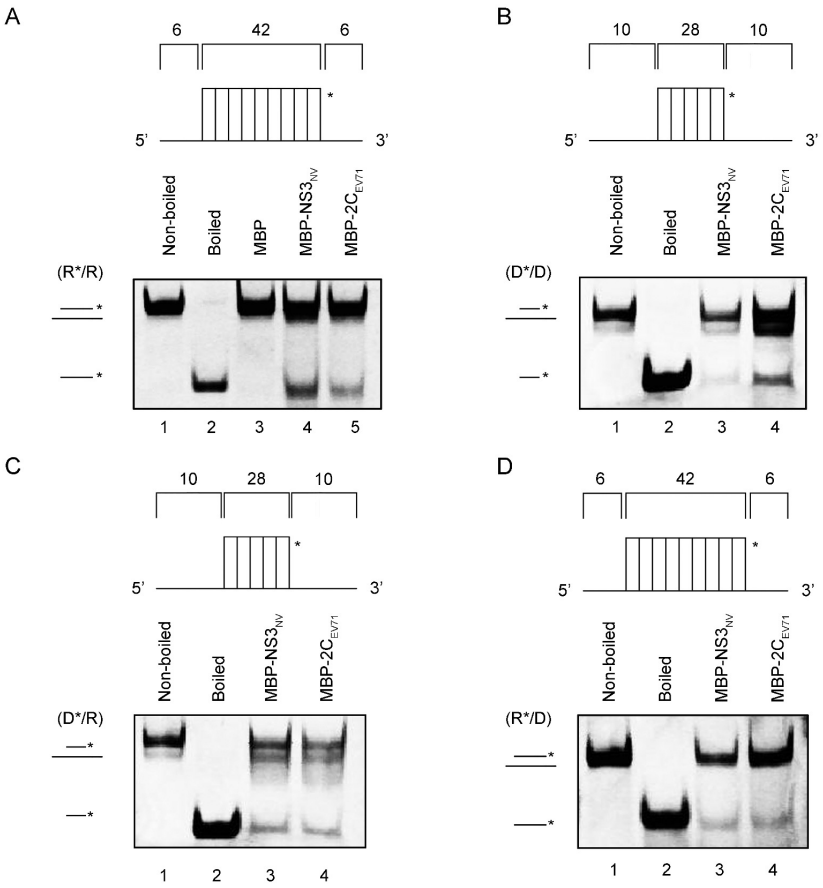

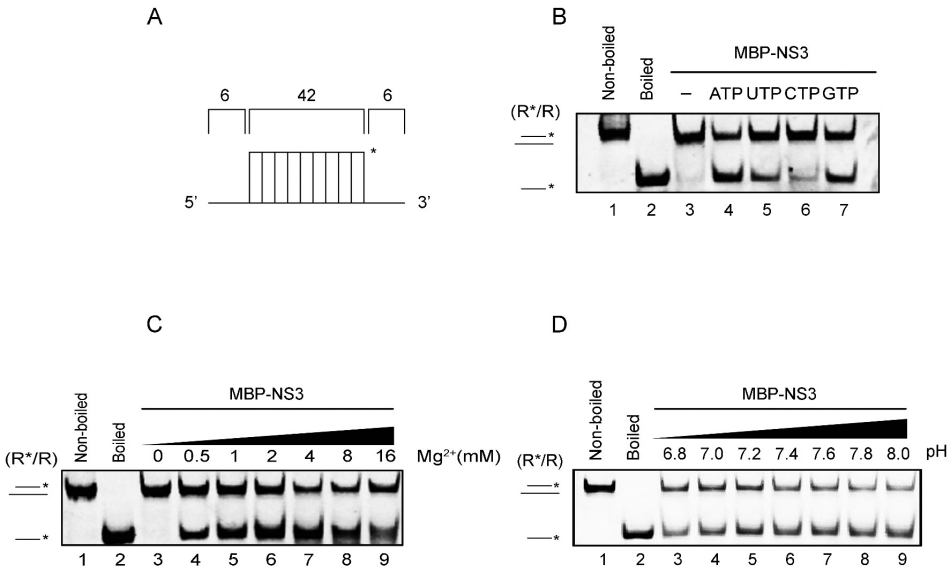

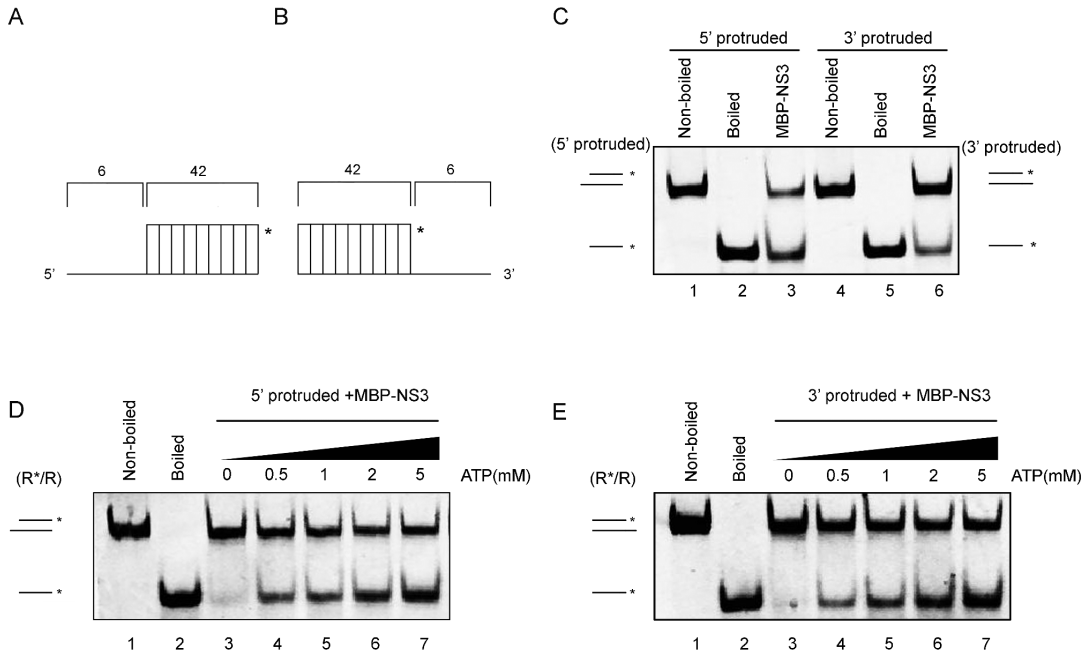

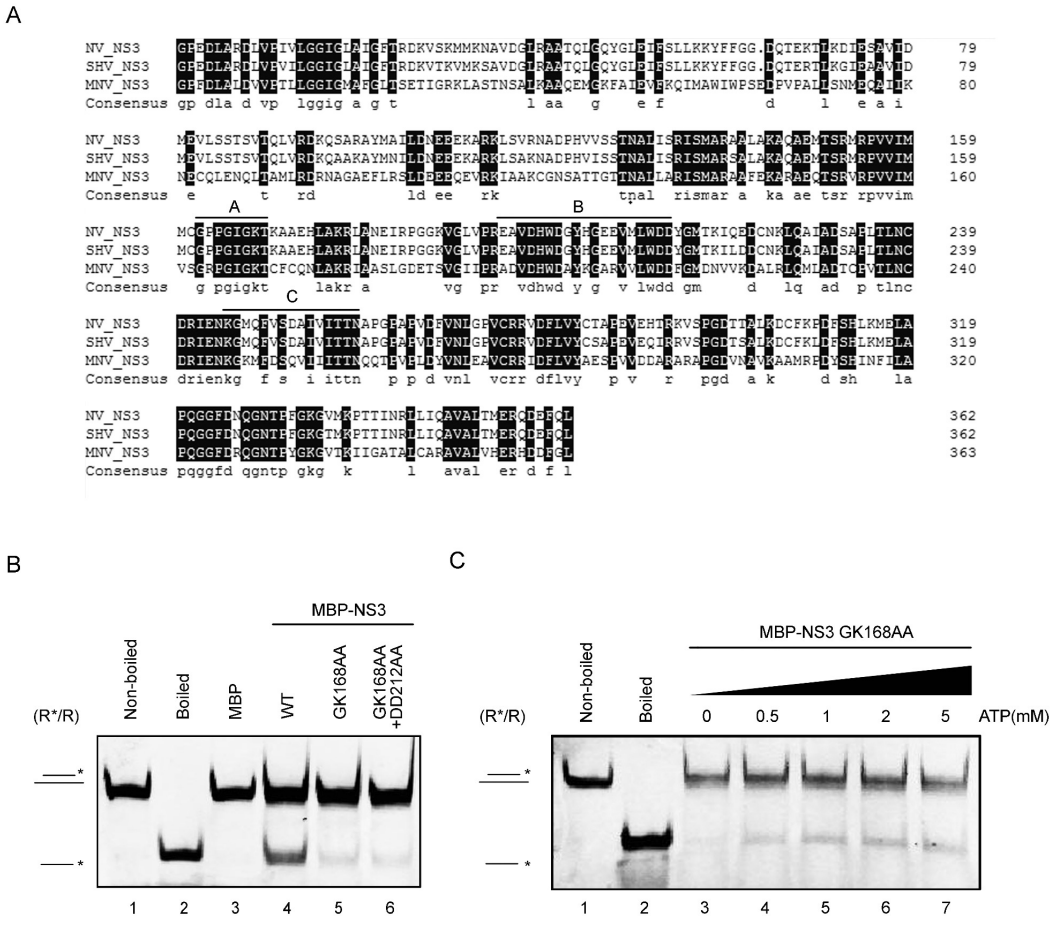

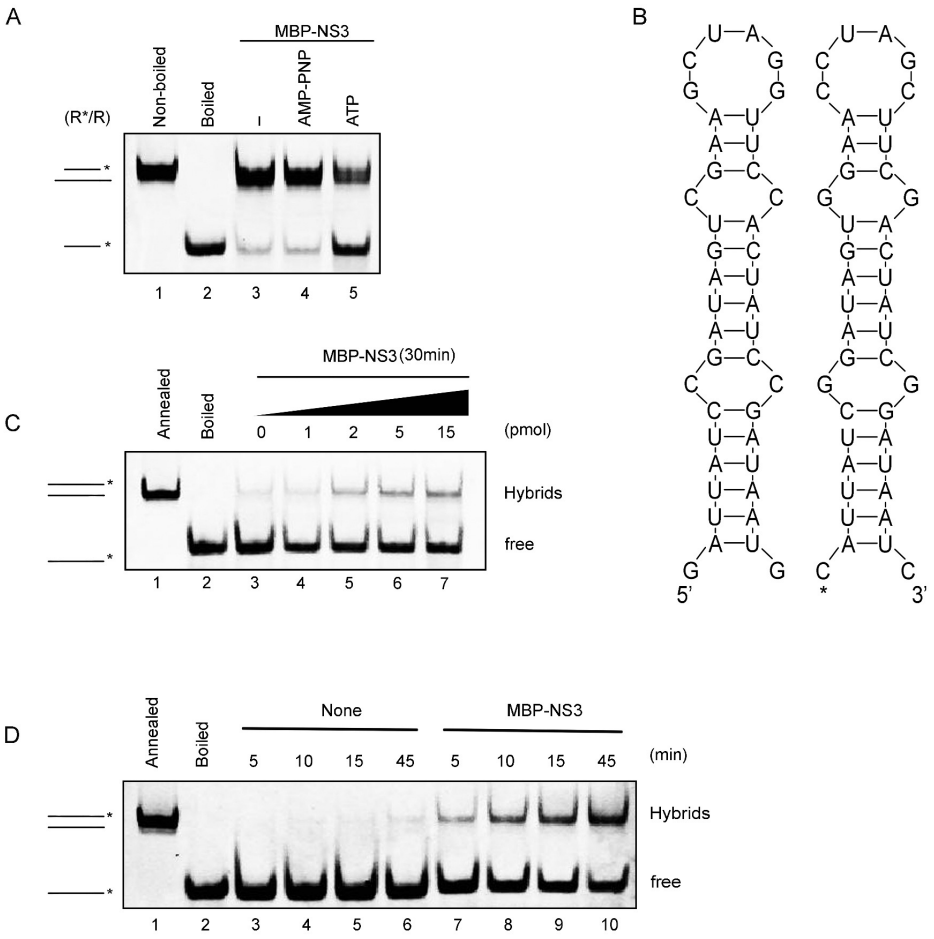

A

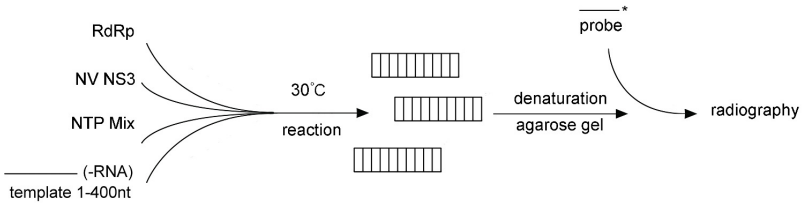

B

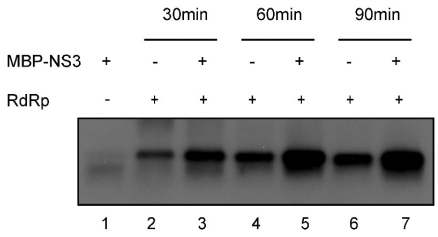

D

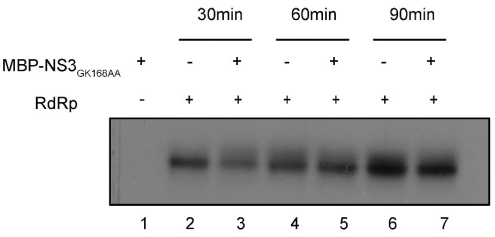

C

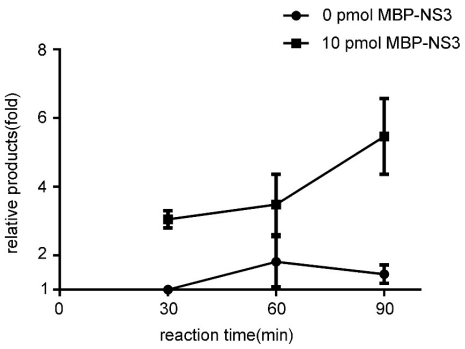

E